

Electronic Supplementary Information (ESI)

Atropisomers and a copper(II) complex derived from 1,3-dimethyl-5-(8'-quinolinylazo)-6-aminouracil: structures, magnetism and biological properties

Nishithendu Bikash Nandi^a, Nisan Das^a, Susanta Ghanta^a, Krishti Rekha Puzari^b, Pranab Dutta^b, Julia Kłak^{*c}, Lesław Sieroń^d, Waldemar Maniukiewicz^{*d}, Tarun Kumar Misra^{*a}

^aDepartment of Chemistry, National Institute of Technology Agartala, Tripura 799046, India

^bSchool of Crop Protection, College of Post Graduate Studies in Agricultural Sciences, Central Agricultural University, Meghalaya, India

^cFaculty of Chemistry, University of Wrocław, Wrocław 50383, Poland

^dInstitute of General and Ecological Chemistry, Łódź University of Technology, Łódź 90924, Poland

Contents

Figures/Tables	Pages
Figure S1. UV-Vis spectra for monitoring conversion of H ₂ L to β -isomer in presence of Cu ²⁺ .	2
Figure S2. FT-IR spectrum of H ₂ L (1).	2
Figure S3. FT-IR spectrum of α -atropisomer(2) of 8-azaxanthine.	3
Figure S4. FT-IR spectrum of Cu(II)-complex (4).	3
Figure S5. Hydrogen bond interactions existed in (a) α -atropisomer, (b) β -atropisomer.	4
Figure S6. Molecular packing of of α -atropisomer (2) of 8-azaxanthine.	4
Figure S7. Molecular packing of β -atropisomer (3) of azaxanthine.	5
Figure S8. H-bonding guided molecular assemble of Cu(II)-complex.	5
Figure S9. Molecular packing of of Cu(II)-Complex, 4 .	6
Figure S10. ¹ H NMR spectrum of H ₂ L.	6
Figure S11. ¹ H NMR spectrum of α -atropisomer (2) of 8-azaxanthine.	7
Figure S12. ¹³ C NMR spectrum of H ₂ L.	7
Figure S13. ¹³ C NMR spectrum of α -atropisomer (2) of 8-azaxanthine.	8
Figure S14. The field dependence of the magnetization (<i>M</i> per one Cu ^{II} cation) at 2 K for 4 . The solid line is the Brillouin function curve for one uncoupled spin with <i>S</i> = 1/2 and <i>g</i> = 2.0.	8
Figure S15. The powder EPR (X-band) spectrum of 4 at 77 K.	9
Table S1. Assigned stretching frequencies of all the synthesized compounds.	9
Table S2. Bond length of atropisomers of 8-azaxanthine and Cu(II)-complex of H ₂ L.	10
Table S3. Bond angles of atropisomers of 8-azaxanthine and Cu(II)-complex of H ₂ L.	11-12

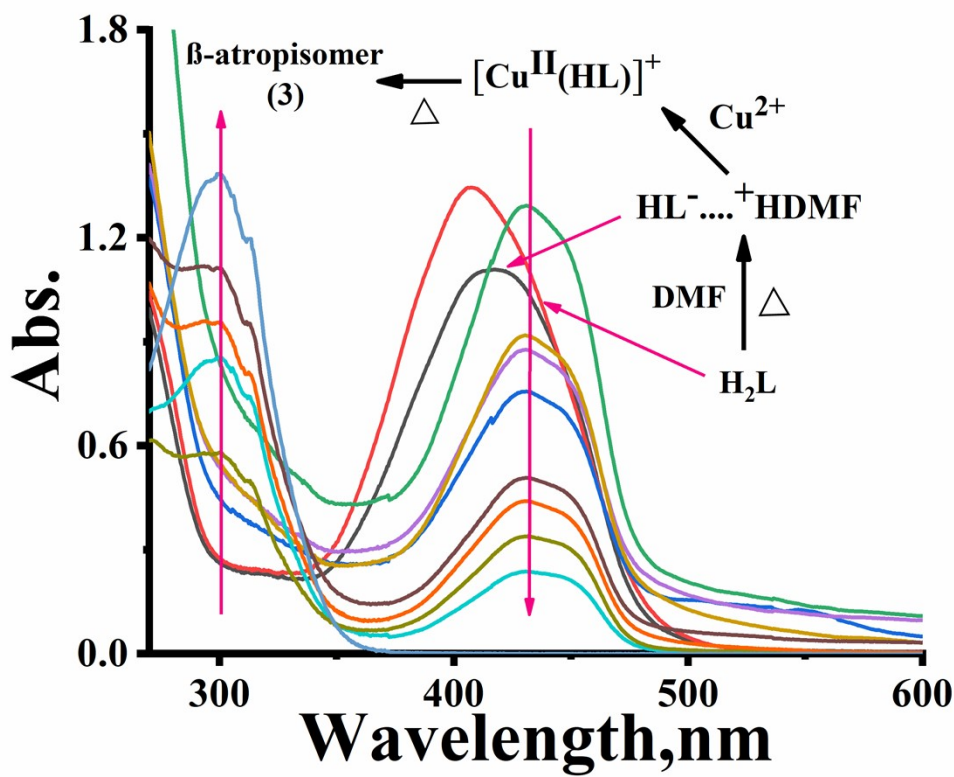


Figure S1. UV-Vis spectra for monitoring conversion of H_2L to β -isomer in presence of Cu^{2+} .

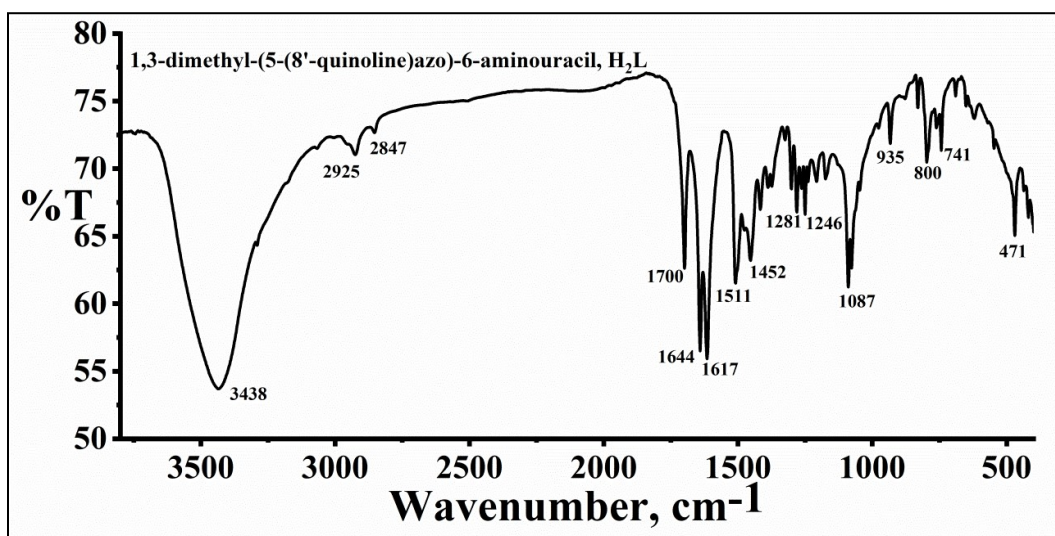


Figure S2. FT-IR spectrum of H_2L (1).

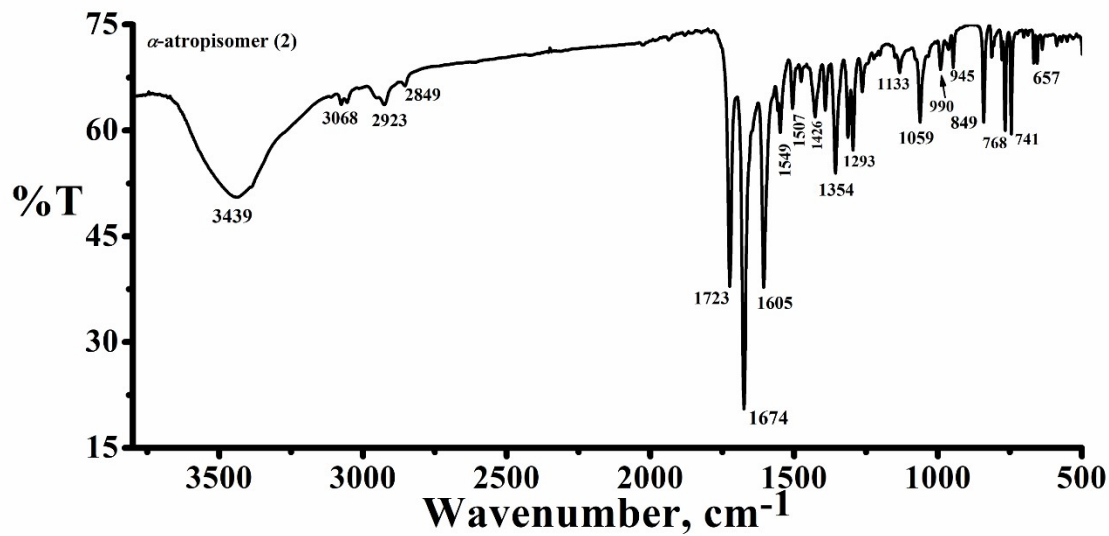


Figure S3. FT-IR spectrum of α -atropisomer(2) of 8-azaxanthine.

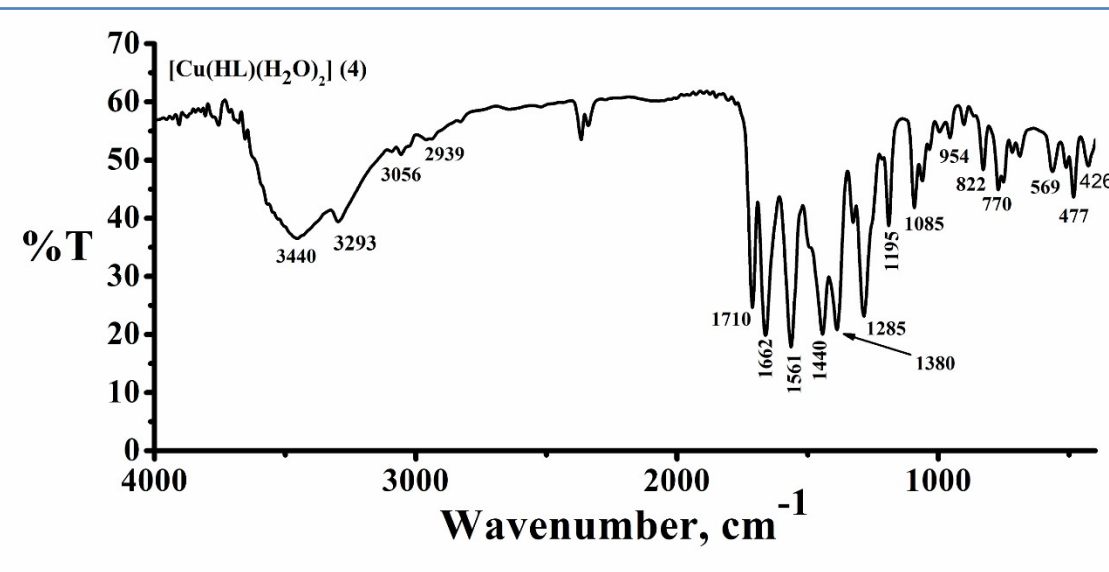


Figure S4. FT-IR spectrum of Cu(II)-complex (4).

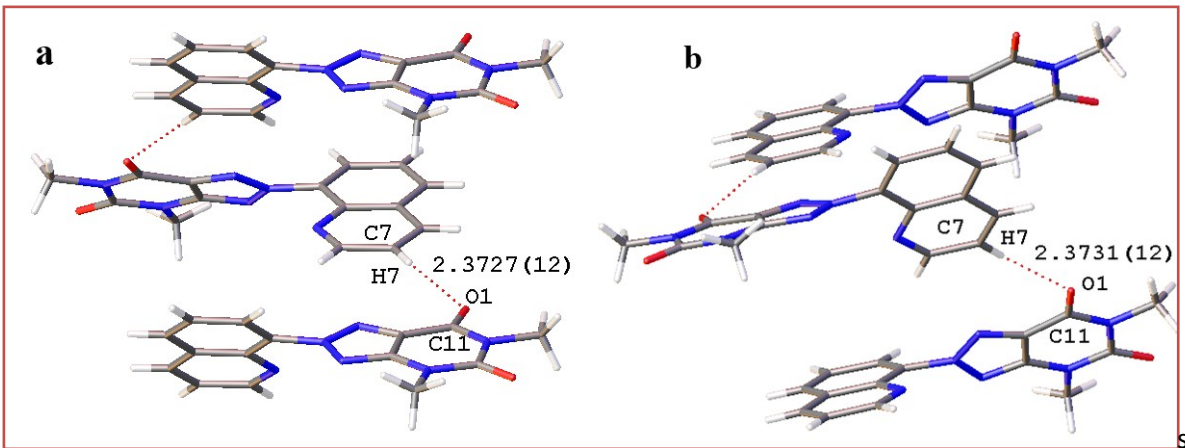


Figure S5. Hydrogen bond interactions existed in (a) α -atropisomer, (b) β -atropisomer.

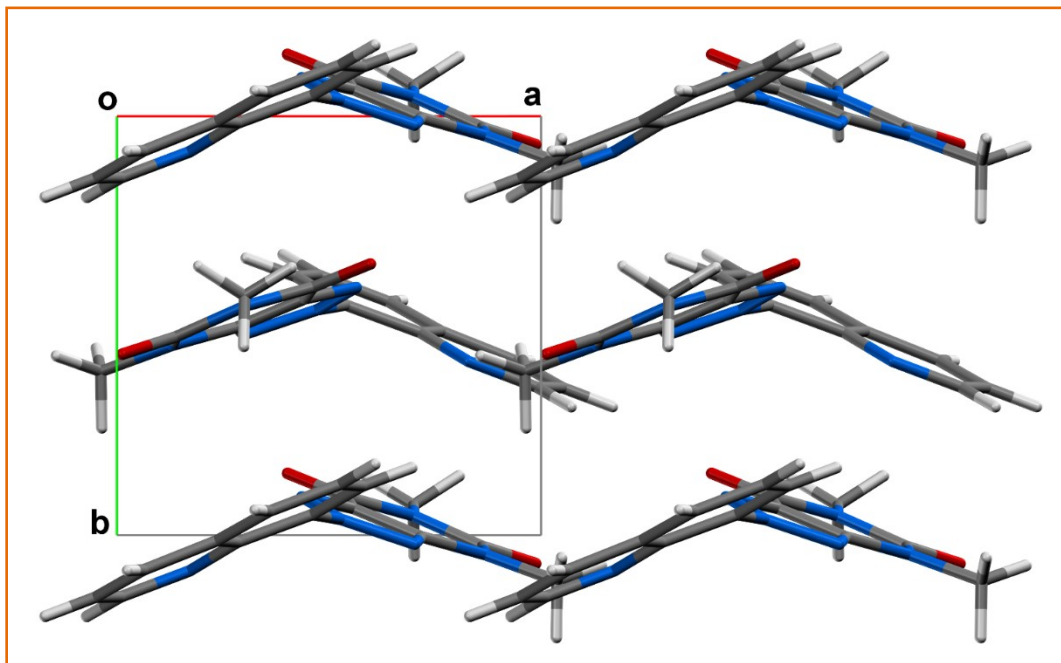


Figure S6. Molecular packing of α -atropisomer (2) of 8-azaxanthine

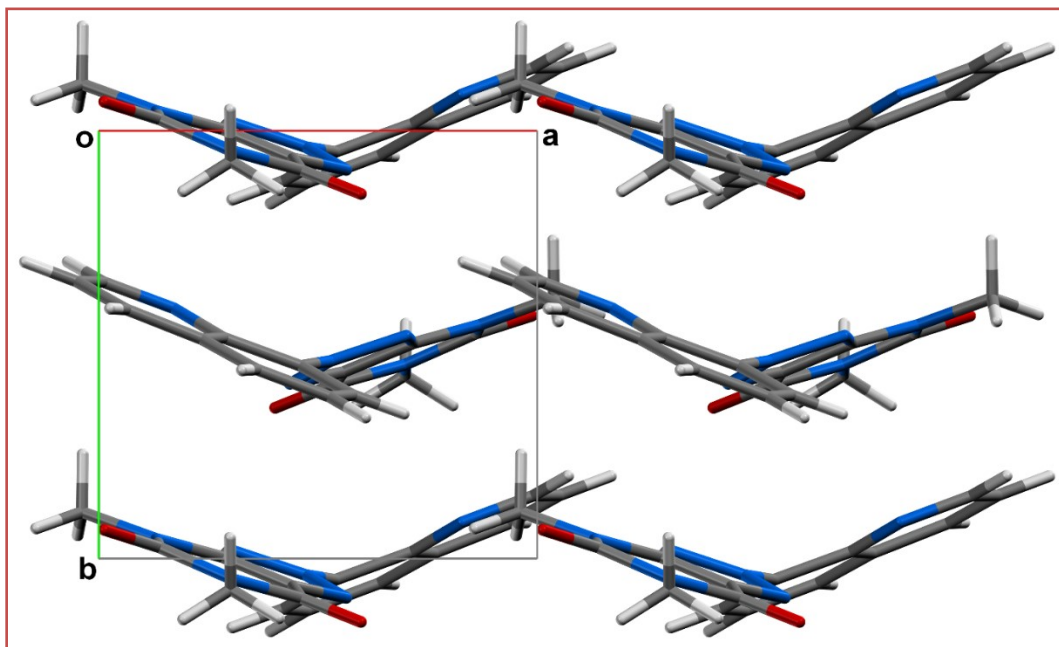


Figure S7. Molecular packing of β -atropisomer (**3**) of azaxanthine.

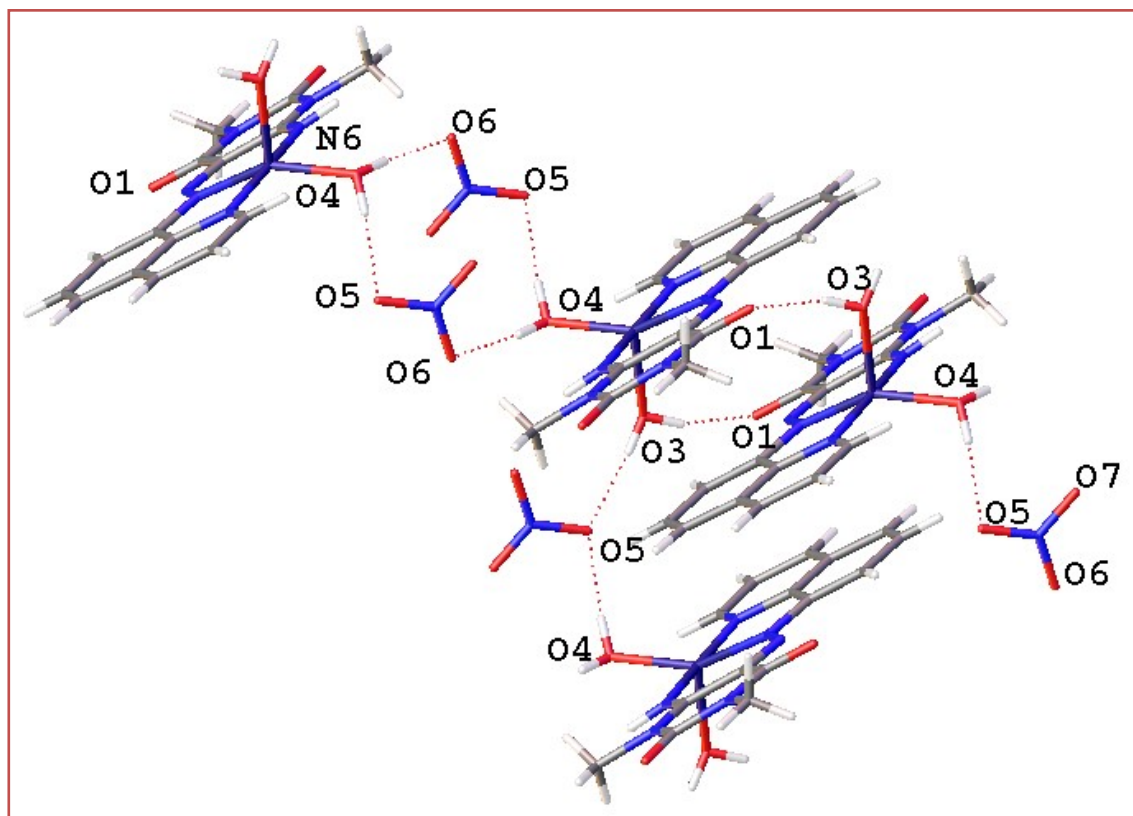


Figure S8. H-bonding guided molecular assemble of Cu(II)-complex.

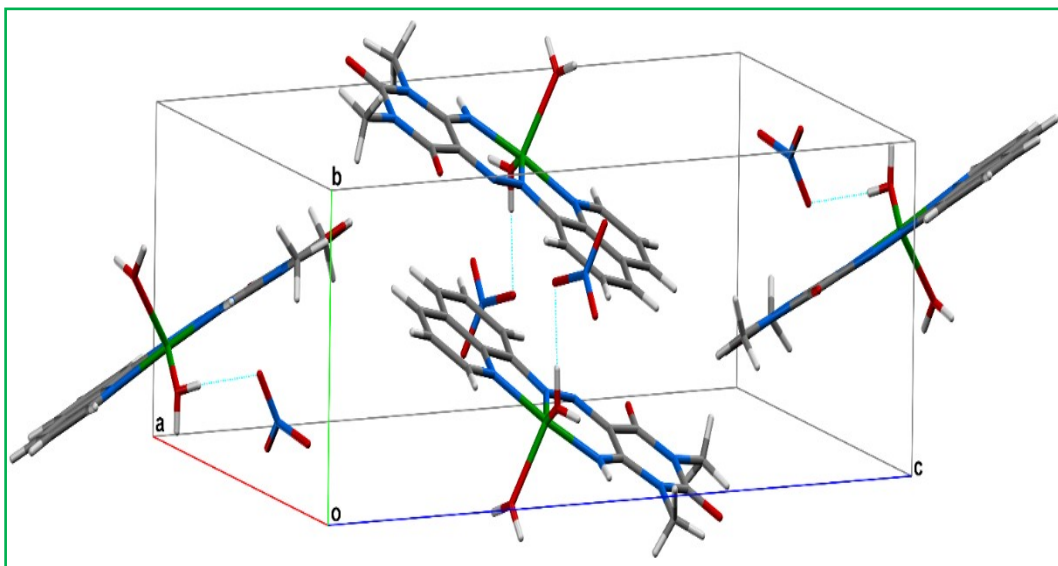


Figure S9. Molecular packing of of Cu(II)-Complex, 4.

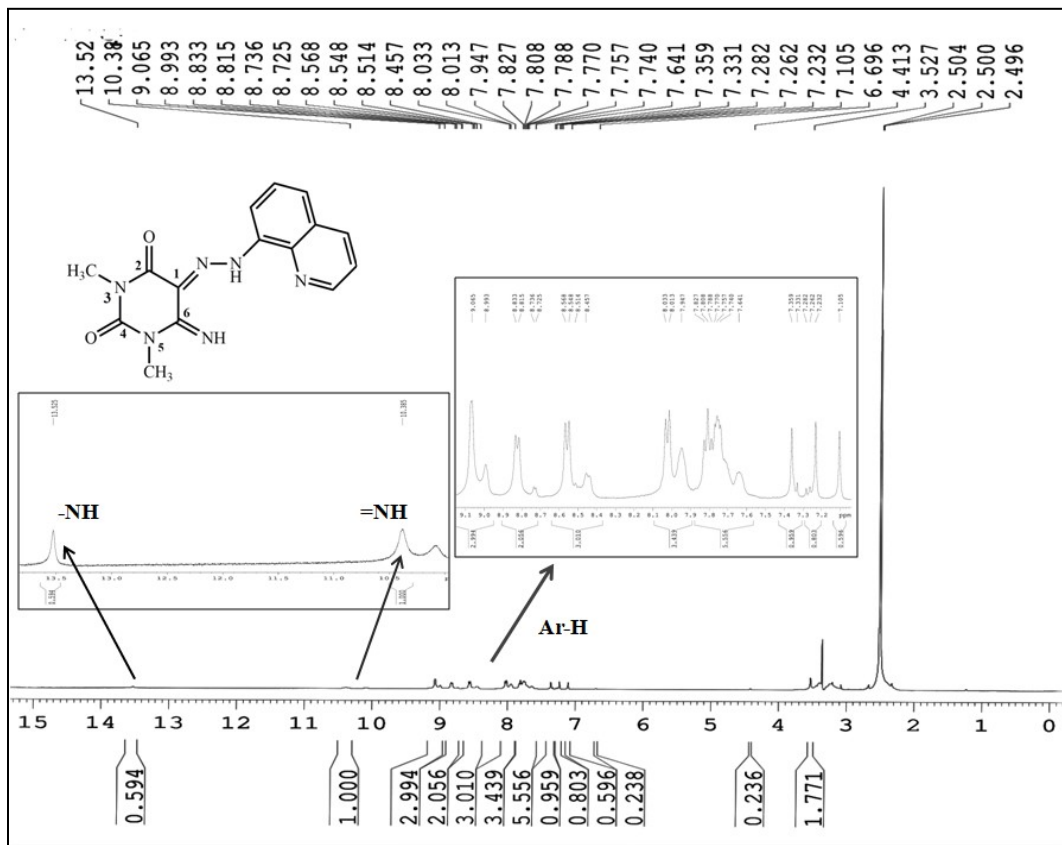


Figure S10. ^1H NMR spectrum of H_2L .

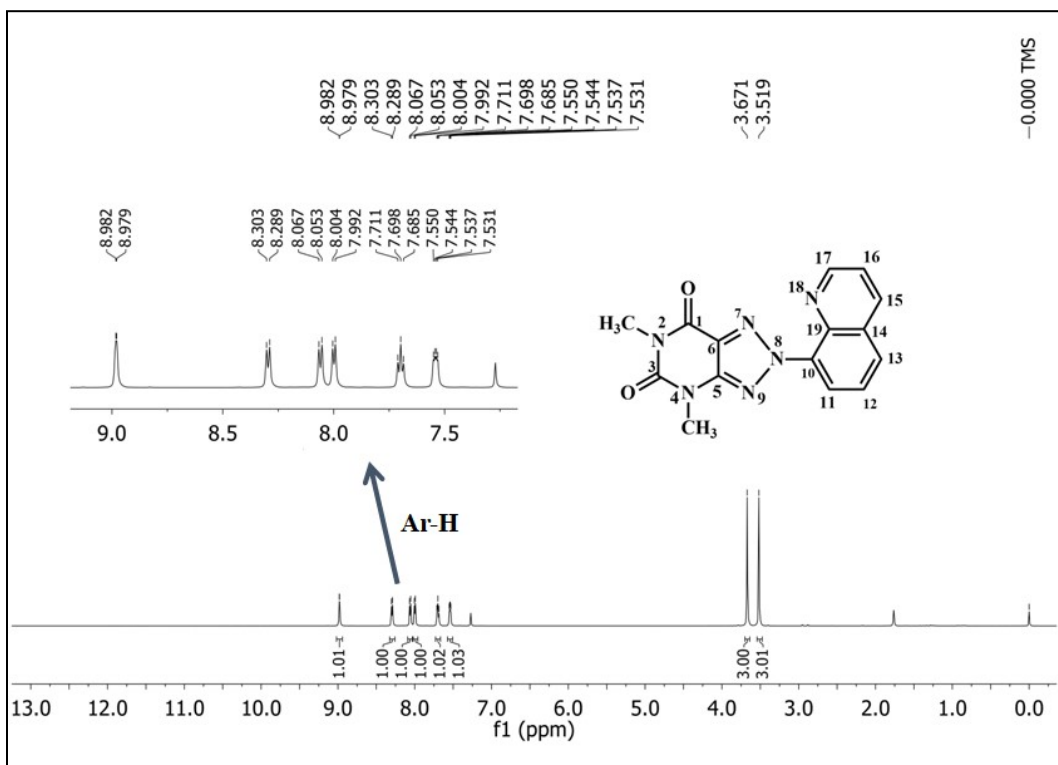


Figure S11. ^1H NMR spectrum of α -atropisomer (**2**) of 8-azaxanthine.

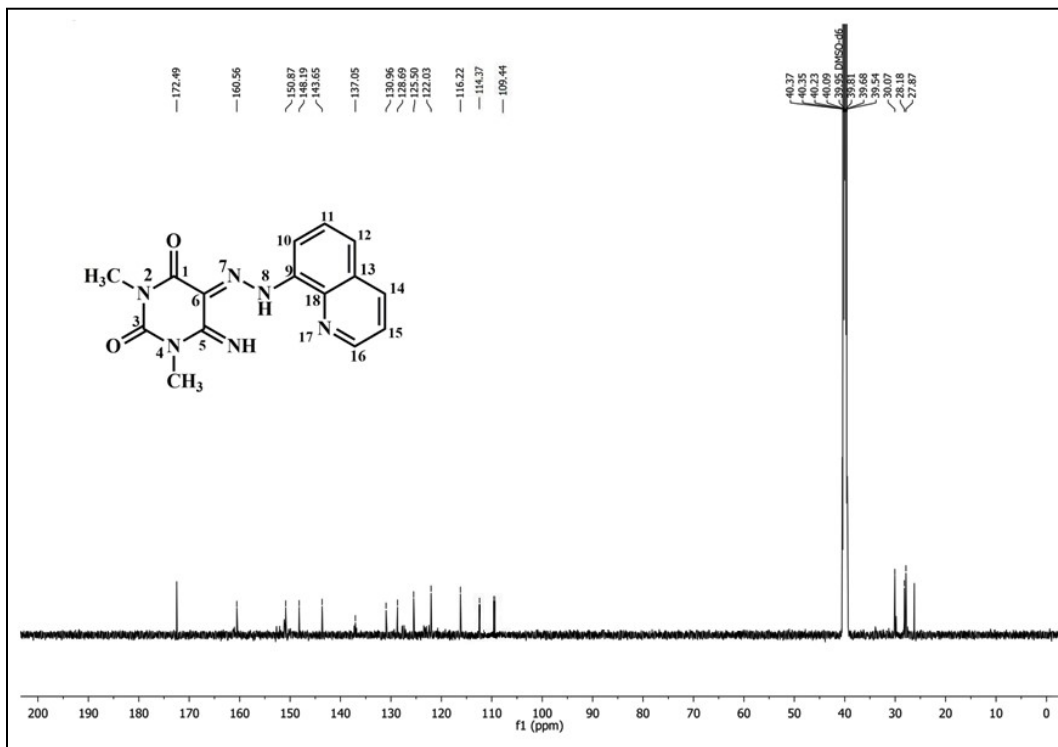


Figure S12. ^{13}C NMR spectrum of H_2L .

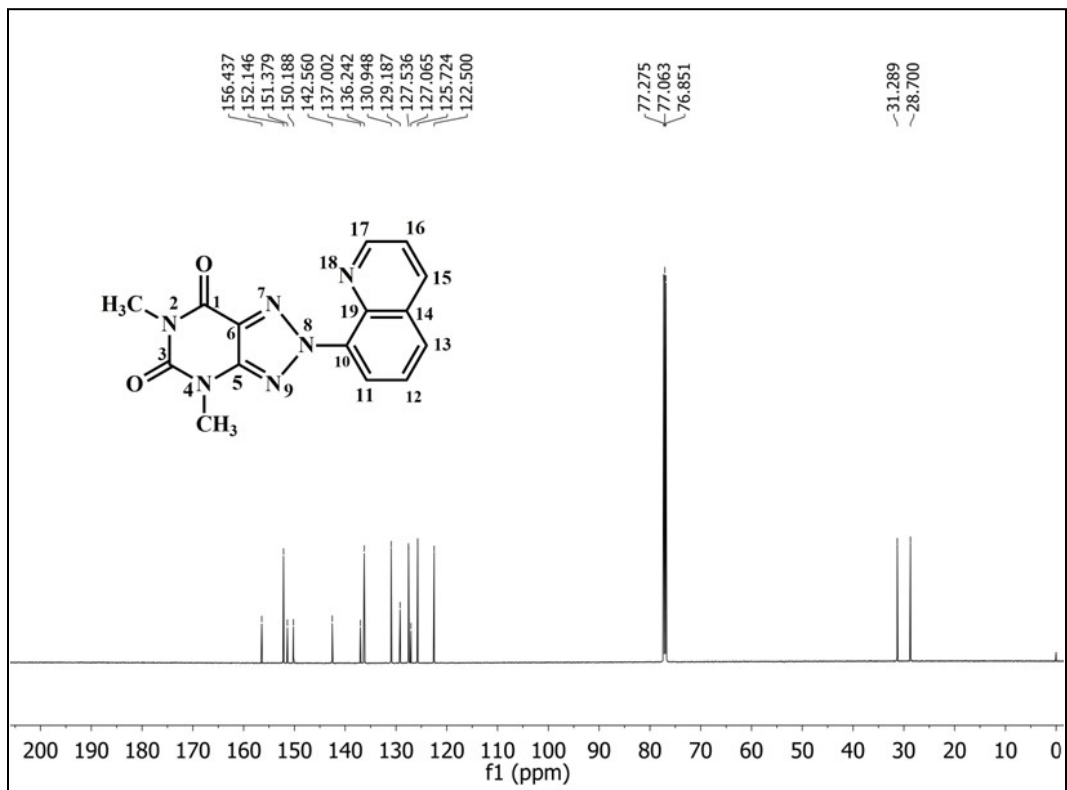


Figure S13. ^{13}C NMR spectrum of α -atropisomer (**2**) of 8-azaxanthine.

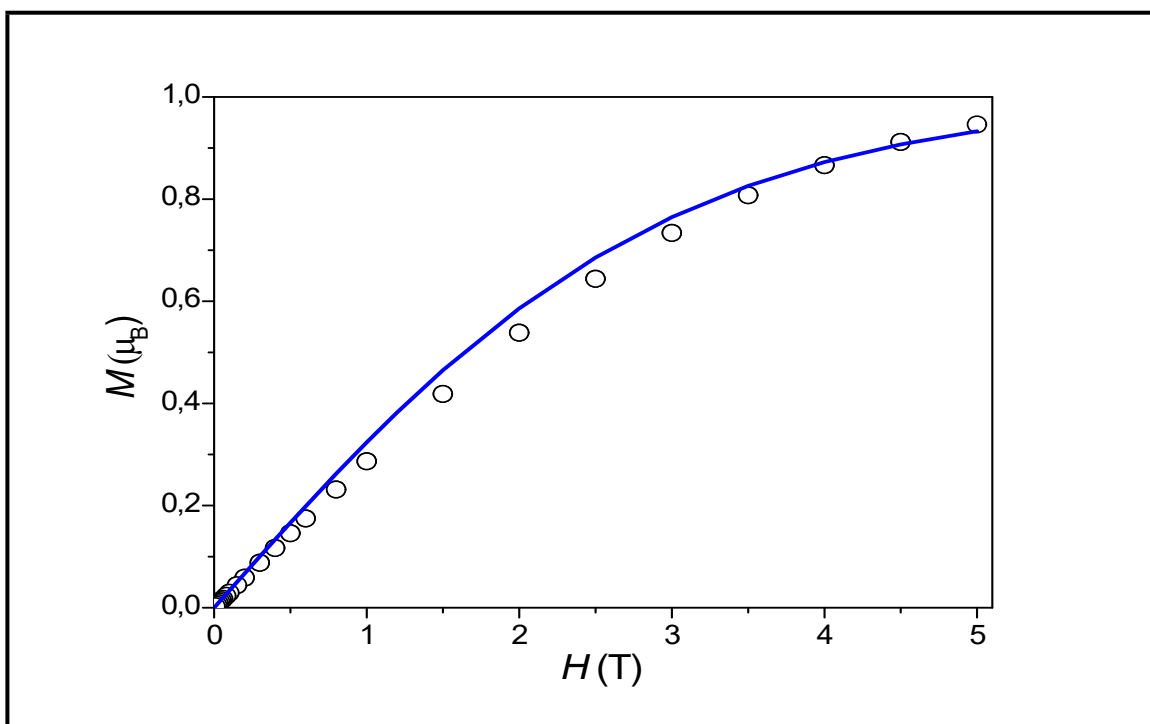


Figure S14. The field dependence of the magnetization (M per one Cu^{II} cation) at 2 K for **4**. The solid line is the Brillouin function curve for one uncoupled spin with $S = 1/2$ and $g = 2.0$.

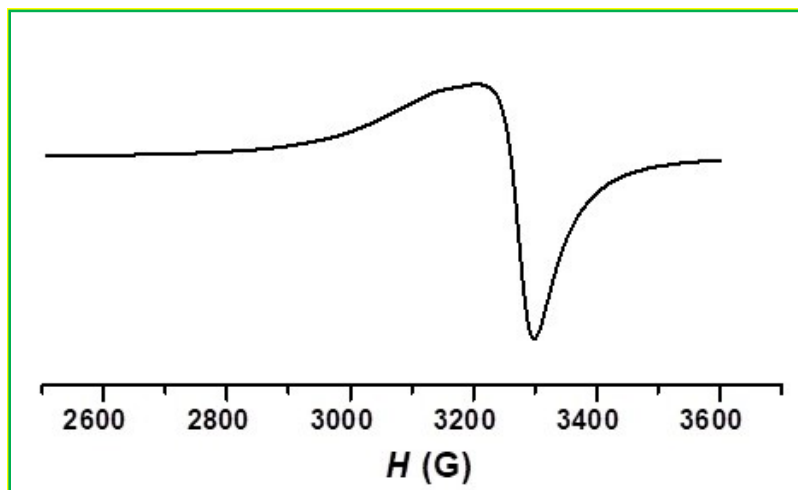


Figure S15. The powder EPR (X-band) spectrum of **4** at 77 K.

Table S1. Assigned stretching frequencies of all the synthesised compounds.

Functional groups	Ligand, H_2L	8-Azaxanthine (α -atropisomer)	Cu(II)-Complex
-NH and Ar-H	3438, 2925, 2847	3439, 3068, 2923, 2849	3440, 3293 , 3056, 2939
$>^2\text{C=O}$	1700	1723	1710
$>^4\text{C=O}$	1644	1674	1662
$-\text{C}=\text{N}/-\text{C}=\text{C}-$	1617	1605	1561
$-\text{N}=\text{N}-$	1452	-	1462
$-\text{C}-\text{O}$	1281	1293	1285
$-\text{C}-\text{C}-$	1246		1195
$-\text{C}-\text{N}-$	1087		1085
$-\text{N}-\text{C}_{\text{bend}}$	-	1354	-
$\text{N}-\text{C}_{\text{stret}}$	-	1059	-
Other bands	935, 800, 741, 471	990, 849, 768, 741, 657	954, 822, 770, 569, 477

Table S2. Bond length of atropisomers of 8-azaxanthine and Cu(II)-complex of H₂L.

1,3-dimethyl-8-(8'-quinolinyl)azaxanthine				Cu(II)-Complex (4)	
α -atropisomer (2)		β -atropisomer (3)			
Bond	Length/Å	Bond	Length/Å	Bond	Length/Å
O1-C11	1.217(2)	O1-C11	1.2180(19)	Cu1-O3	2.2207(13)
O2-C12	1.214(2)	O2-C12	1.215(2)	Cu1-O4	2.0570(12)
N1-C8	1.330(2)	N1-C8	1.328(2)	Cu1-N1	1.9837(15)
N1-C9	1.366(2)	N1-C9	1.366(2)	Cu1-N2	1.9557(15)
N2-N3	1.327(2)	N2-N3	1.3277(19)	Cu1-N6	1.9211(15)
N2-N4	1.362(2)	N2-N4	1.3616(19)	O1-C11	1.225(2)
N2-C1	1.432(2)	N2-C1	1.432(2)	O2-C12	1.220(2)
N3-C10	1.343(2)	N3-C10	1.343(2)	N1-C8	1.331(2)
N4-C13	1.325(2)	N4-C13	1.325(2)	N1-C9	1.365(2)
N5-C11	1.403(2)	N5-C11	1.403(2)	N2-N3	1.297(2)
N5-C12	1.409(2)	N5-C12	1.409(2)	N2-C1	1.413(2)
N5-C14	1.471(2)	N5-C14	1.472(2)	N3-C10	1.340(2)
N6-C12	1.380(2)	N6-C12	1.380(2)	N4-C11	1.391(2)
N6-C13	1.374(2)	N6-C13	1.372(2)	N4-C12	1.380(2)
N6-C15	1.467(2)	N6-C15	1.466(2)	N4-C14	1.469(2)
C1-C2	1.371(2)	C1-C2	1.372(2)	N5-C12	1.389(2)
C1-C9	1.424(2)	C1-C9	1.424(2)	N5-C13	1.392(2)
C2-C3	1.411(3)	C2-C3	1.410(2)	N5-C15	1.468(2)
C3-C4	1.366(3)	C3-C4	1.365(2)	N6-C13	1.296(2)
C4-C5	1.419(3)	C4-C5	1.418(2)	C1-C2	1.369(2)
C5-C6	1.414(2)	C5-C6	1.415(2)	C1-C9	1.425(2)
C5-C9	1.427(2)	C5-C9	1.428(2)	C2-C3	1.412(2)
C6-C7	1.364(2)	C6-C7	1.364(2)	C3-C4	1.377(3)
C7-C8	1.410(3)	C7-C8	1.411(3)	C4-C5	1.419(3)
C10-C11	1.452(2)	C10-C11	1.450(2)	C5-C6	1.415(2)
C10-C13	1.389(2)	C10-C13	1.390(2)	C5-C9	1.413(2)
				O5-N7	1.2742(19)
				C6-C7	1.370(3)
				O6-N7	1.2570(19)
				C7-C8	1.402(3)
				O7-N7	1.2336(19)
				C10-C11	1.462(2)
				C10-C13	1.442(2)

Table S3. Bond angles of atropisomers of 8-azaxanthine and Cu(II)-complex of H₂L.

1,3-dimethyl-8-(8'-quinolinyl)azaxanthine				Cu(II)-Complex (4)	
α -atropisomer (2)		β -atropisomer (3)			
Bond	Angle /°	Bond	Angle /°	Bond	Angle /°
C8-N1-C9	116.83(15)	C8-N1-C9	116.86(14)	O3-Cu1-O4	86.46(5)
N3-N2-N4	116.69(13)	N3-N2-N4	116.64(13)	O3-Cu1-N1	87.68(5)
N3-N2-C1	124.85(14)	N3-N2-C1	124.83(13)	O3-Cu1-N2	120.49(5)
N4-N2-C1	118.35(13)	N4-N2-C1	118.42(13)	O3-Cu1-N6	98.12(5)
N2-N3-C10	102.39(13)	N2-N3-C10	102.38(13)	O4-Cu1-N1	92.57(6)
N2-N4-C13	101.50(13)	N2-N4-C13	101.58(13)	O4-Cu1-N2	152.31(6)
C11-N5-C12	127.98(15)	C11-N5-C12	127.96(13)	O4-Cu1-N6	92.95(6)
C11-N5-C14	116.93(15)	C11-N5-C14	116.93(14)	N1-Cu1-N2	83.08(6)
C12-N5-C14	115.06(15)	C12-N5-C14	115.09(14)	N1-Cu1-N6	172.23(6)
C12-N6-C13	118.92(14)	C12-N6-C13	118.92(14)	N2-Cu1-N6	89.50(6)
C12-N6-C15	120.02(14)	C12-N6-C15	120.01(14)	Cu1-N1-C8	128.49(13)
C13-N6-C15	121.05(14)	C13-N6-C15	121.06(14)	Cu1-N1-C9	112.60(11)
N2-C1-C2	116.80(14)	N2-C1-C2	116.76(14)	C8-N1-C9	118.82(15)
N2-C1-C9	121.10(14)	N2-C1-C9	121.17(14)	Cu1-N2-N3	131.21(12)
C2-C1-C9	122.01(15)	C2-C1-C9	121.96(15)	Cu1-N2-C1	113.62(11)
C1-C2-C3	119.97(15)	C1-C2-C3	119.97(14)	N3-N2-C1	115.13(14)
C2-C3-C4	120.40(16)	C2-C3-C4	120.46(15)	N2-N3-C10	120.82(15)
C3-C4-C5	120.44(16)	C3-C4-C5	120.42(15)	C11-N4-C12	125.10(14)
C4-C5-C6	122.12(16)	C4-C5-C6	122.20(15)	C11-N4-C14	117.65(15)
C4-C5-C9	120.29(15)	C4-C5-C9	120.30(14)	C12-N4-C14	117.23(14)
C6-C5-C9	117.60(14)	C6-C5-C9	117.50(14)	C12-N5-C13	124.41(15)
C5-C6-C7	119.31(17)	C5-C6-C7	119.35(16)	C12-N5-C15	116.73(14)
C6-C7-C8	118.99(16)	C6-C7-C8	118.95(15)	Cu1-N6-C13	128.58(12)
N1-C8-C7	124.42(16)	N1-C8-C7	124.47(16)	N2-C1-C2	127.01(15)
N1-C9-C1	120.24(15)	N1-C9-C1	120.24(15)	N2-C1-C9	113.52(14)
N1-C9-C5	122.85(14)	N1-C9-C5	122.86(14)	C2-C1-C9	119.47(15)
C1-C9-C5	116.88(14)	C1-C9-C5	116.88(14)	C13-N5-C15	118.78(14)
N3-C10-C11	129.38(15)	N3-C10-C11	129.38(15)	C1-C2-C3	120.39(16)
N3-C10-C13	109.06(15)	N3-C10-C13	109.09(14)	C2-C3-C4	121.17(16)
C11-C10-C13	121.56(15)	C11-C10-C13	121.52(15)	C3-C4-C5	119.77(16)
O1-C11-N5	122.35(16)	O1-C11-N5	122.30(15)	C4-C5-C6	124.50(16)
O1-C11-C10	126.55(15)	O1-C11-C10	126.55(15)	C4-C5-C9	118.85(15)
N5-C11-C10	111.10(14)	N5-C11-C10	111.14(13)	C6-C5-C9	116.65(16)

O2-C12-N5	120.66(16)	O2-C12-N5	120.65(15)	C5-C6-C7	120.36(17)
O2-C12-N6	122.28(15)	O2-C12-N6	122.32(15)	C6-C7-C8	119.15(17)
N5-C12-N6	117.05(14)	N5-C12-N6	117.02(14)	N1-C8-C7	122.46(17)
N4-C13-N6	126.35(15)	N4-C13-N6	126.38(14)	N1-C9-C1	117.12(15)
N4-C13-C10	110.37(15)	N4-C13-C10	110.31(14)	N1-C9-C5	122.57(15)
N6-C13-C10	123.28(16)	N6-C13-C10	123.31(15)	C1-C9-C5	120.32(16)
				N3-C10-C11	112.73(15)
				N3-C10-C13	127.05(15)
				C11-C10-C13	120.22(14)
				O1-C11-N4	119.05(15)
				O1-C11-C10	124.75(15)
				N4-C11-C10	116.20(15)
				O2-C12-N4	121.66(17)
				O2-C12-N5	121.43(17)
				N4-C12-N5	116.91(14)
				N5-C13-N6	120.20(15)
				N4-C13-C10	117.09(14)
				N6-C13-C10	122.71(15)
				O5-N7-O6	118.80(14)
				O5-N7-O7	119.87(14)
				O6-N7-O7	121.34(15)
Atoms	Torsion Angle (°)	Atoms	Torsion Angle (°)	Atoms	Torsion Angle (°)
N3-N2-C1-C9	48.7(2)	N3-N2-C1-C9	-48.7(2)	Cu1-N1-C8-C7	-176.93(14)
N3-N2-N4-C13	-0.32(19)	N3-N2-N4-C13	0.32(18)	Cu1-N1-C9-C1	-2.60(18)
C6-C5-C9-C1	-178.25(15)	C6-C5-C9-C1	178.28(15)	Cu1-N1-C9-C5	177.39(12)
C9-C5-C6-C7	-0.9(3)	C9-C5-C6-C7	1.0(3)	Cu1-N2-N3-C10	0.4(2)
C13-N6-C12-N5	3.2(3)	C13-N6-C12-N5	-3.3(2)	Cu1-N2-C1-C9	0.94(17)
C3-C4-C5-C6	179.12(19)	C3-C4-C5-C6	-179.16(19)	Cu1-N6-C13-C10	-4.4(2)
N4-N2-C1-C9	-135.41(15)	N4-N2-C1-C9	135.33(15)	O3-Cu1-N1-C8	57.67(15)
N3-C10-C11-O1	-0.1(4)	N3-C10-C11-O1	0.1(3)	O3-Cu1-N2-C1	81.35(12)
C4-C5-C9-N1	179.05(16)	C4-C5-C9-N1	-179.01(16)	N2-Cu1-N1-C9	2.40(11)
C14-N5-C11-O1	1.1(3)	C14-N5-C11-O1	-1.1(2)	N1-Cu1-N2-C1	-1.82(11)